PAPR Reduction for Bit-loaded OFDM in Visible Light Communications

Zhenhua Yu[1], Kai Ying[2], Robert J. Baxley[3] and G. Tong Zhou[2]
[1] Texas Instruments, 12500 TI Boulevard MS 8649, Dallas, TX 75243, USA
[2] Georgia Institute of Technology, Atlanta, GA 30332, USA
[3] Bastille Networks, 1000 Marietta St # 112, Atlanta, GA 30318, USA
Email: z-yu3@ti.com

***Abstract*—Visible light communications (VLC) rely on white light emitting diodes (LEDs) to provide communication and illumination simultaneously. Orthogonal frequency division multiplexing (OFDM) enables bit loading in VLC to make the best use of available modulation bandwidth of white LEDs. However, OFDM signals in VLC exhibit high peak-to-average power ratio (PAPR) as in radio frequency (RF) communications. VLC-OFDM differs from RF-OFDM in that the baseband signals are real-valued and there are two PAPRs to be reduced, namely upper PAPR and lower PAPR. Moreover, upper PAPR and lower PAPR are not independently distributed, and are often subject to asymmetric constraints. In this paper, we propose a distortion-based PAPR reduction scheme to minimize the weighted upper PAPR and lower PAPR in VLC-OFDM. The proposed method takes bit loading into consideration that ensures allocating less distortions to subcarriers with more bits loaded (higher order constellations).**

I. Introduction

Visible light communications (VLC) leverage white light emitting diodes (LEDs) to provide "green communication" by simple and low-cost intensity modulation and direct detection (IM/DD) techniques. VLC can help address the current challenges in wireless communications such as the bandwidth limitation, energy efficiency, electromagnetic interference and safety [1], [2]. VLC draw more and more attentions recently and are on the road to commercialization [3].

Limited modulation bandwidth of LED is one of challenges in VLC [4]. VLC channel exhibits frequency-selectivity due to the low-pass filter characteristics of LEDs. Conventional single carrier modulations, such as on-off keying (OOK), pulse-position modulation (PPM), and pulse-amplitude modulation (PAM), suffer from the frequency-selective channel as data rates increase. To best make use of available bandwidth of LEDs and boost the achievable data rates, orthogonal frequency division multiplexing (OFDM) has been considered for VLC [5]–[7]. Specifically, bit-loaded OFDM systems allow allocating different numbers of bits to different subcarriers based on signal-to-noise power ratio (SNR) [8], [9]. With bit loading techniques, OFDM enables more than 3-dB modulation bandwidth of LEDs.

VLC-OFDM holds the disadvantage of high peak-to-average power ratio (PAPR) as the radio frequency (RF) OFDM [10]. The major difference between VLC-OFDM and RF-OFDM is that IM/DD requires the VLC-OFDM baseband signal to be real-valued and unipolar (positive-valued). Therefore, in VLC-OFDM, Hermitian symmetry must be satisfied in the frequency-domain and bipolar-to-unipolar module is required. In RF-OFDM, PAPR reduction is motivated by mitigating nonlinear distortions caused by power amplifiers (PAs) and increasing the power efficiency of PAs. In VLC, the nonlinear source becomes LEDs [11]. In addition, high PAPR requires large biasing to convert the bipolar OFDM signal into unipolar version, which makes the system optical power inefficient [12]. Therefore, PAPR reduction is also an indispensable module in VLC-OFDM system. Among PAPR reduction schemes proposed for RF-OFDM communications [10], the distortion based methods [13]–[18] are in particular favored for practical scenario because the modification of receivers is avoided. However, real-valued VLC-OFDM signals have two PAPRs to be reduced, namely upper PAPR and lower PAPR [19], which prevents directly applying conventional PAPR reduction methods to VLC-OFDM systems. Upper PAPR and lower PAPR are not independently distributed and are often limited by asymmetric constraints. In addition, prior distortion-based PAPR reduction methods only constrain the total distortion power, which results in allocating distortions uniformly onto all in-band subcarriers [15], [16]. However, in bit-loaded OFDM, high-order constellations are often more sensitive to the noise than low-order constellations. Ideally, given a certain amount of distortions, we would like to allocate more distortions to low-order modulations and less distortions to high-order modulations.

To address the PAPR reduction for bit-loaded VLC–OFDM system, we proposed a time-domain impulses injection method (IIM) in reference [20]. But IIM strives to minimize introduced distortions given deterministic PAPR constraints. Unlike IIM, in this paper, we propose a convex-optimization based method to minimize the upper PAPR and lower PAPR given deterministic constellation-wise distortion constraints. The rest of this paper is organized as follows: Section II will review VLC-OFDM systems and bit loading technique. In Section III, we will first investigate the joint distribution of upper and lower PAPR, and then analyze the error vector magnitude (EVM) of clipped OFDM signals. Last, we will formulate the PAPR reduction to a convex optimization problem. Section IV will provide simulation results and Section V will conclude this paper.

II. Bit loaded VLC-OFDM

VLC employ simple and low-cost intensity modulation (IM) and direct detection (DD) schemes. At the transmitter, the forward signal drives the LED which in turn converts the

978-1-4799-8406-0/15/$31.00 ©2015 IEEE

magnitude of the input electric signal into optical intensity. The human eye cannot perceive fast-changing variations of the light intensity, and only responds to the average light intensity. Because communication is "piggyback" on the illumination function, white LEDs are normally adopted to simultaneously provide lighting and communication in VLC. The emitted light by white LEDs includes the whole visible light spectrum from 375 to 780 nm (400 to 800 THz). Phosphorescent LED, which uses the blue LED chip coated with a yellow phosphor, is the most popular white LED in the market due to its low cost. However, the slow response of phosphor limits the 3-dB modulation bandwidth of the phosphorescent white LEDs to only a few MHz. A blue filter can be operated at the receiver to increase the modulation bandwidth to 20 MHz [4]. Thus, the white LED acts as a low-pass filter. At the receiver, a photodiode (PD) transforms the received optical power into the amplitude of an electrical signal.

The whole VLC channel exhibits frequency-selectivity due to the low-pass filter characteristics of white LEDs. OFDM enables the bit loading for each subcarrier to make the best use of the available modulation bandwidth. In an OFDM system, a discrete time-domain symbol sequence $\{x_n\}_{n=0}^{N-1}$ is generated by applying the inverse DFT (IDFT) operation to a frequency-domain sequence $\{X_k\}_{k=-N/2}^{N/2-1}$, where n is the time-domain sample index, k is the frequency-domain subcarrier index, and N is the size of IDFT. However, conventional OFDM cannot be directly used in VLC, because the baseband time-domain signals $\{x_n\}_{n=0}^{N-1}$ are complex-valued, including in-phase and quadrature components. In a VLC system using LED, IM/DD schemes require the input signal of the LED to be real-valued. According to the property of the inverse Fourier transform, a real-valued time-domain signal x_n corresponds to a frequency-domain signal X_k that is Hermitian symmetric; i.e.,

$$X_k \quad = \quad X_{-k}^*, \quad 1 \leq k \leq N/2-1, \tag{1}$$

where $*$ denotes complex conjugate. The 0th and $-N/2$th subcarrier are null; i.e., $X_0 = 0$, $X_{-N/2} = 0$. Then we can obtain the real-valued time-domain signal x_n as

$$\begin{aligned} x_n \quad &= \quad \frac{1}{\sqrt{N}} \sum_{k=-N/2}^{N/2-1} X_k \exp\left(\frac{j2\pi kn}{N}\right) \\ &= \quad \frac{2}{\sqrt{N}} \sum_{k=1}^{N/2-1} \left(\Re(X_k) \cos\left(\frac{2\pi kn}{N}\right) - \right. \\ &\qquad \left. \Im(X_k) \sin\left(\frac{2\pi kn}{N}\right) \right), n = 0, 1, \ldots, N-1, \end{aligned} \tag{2}$$

where $\Re(\cdot)$ denotes the real part of X_k, and $\Im(\cdot)$ denotes the imaginary part of X_k. Since the DC component is zero ($X_0 = 0$), x_n has zero mean and thus is bipolar. However, LEDs place dynamic range constraints $[I_L, I_H]$ on the input driving signals, where I_L denotes the minimum input current to turn on the LED, and I_H denotes the maximum input current to prevent overheating the LED. The input signal that is below the I_L will be clipped. Therefore, the original bipolar OFDM signal x_n has to be converted into unipolar (positive) signal. In this paper, we focus on the DC biased bipolar-to-unipolar conversion scheme, where the input signal of LEDs y_n is obtained via adding a biasing B to the original OFDM signal x_n; i.e.,

$$y_n = x_n + B. \tag{3}$$

Adding a biasing will only affect the DC component X_0, which is not an issue since we do not put data on the DC subcarrier.

In bit-loaded OFDM, the number of bits (constellation) assigned on each subcarrier is determined by the signal to noise power ratio (SNR). For a target bit error rate (BER), the number of bits allocated on the kth subcarrier can be approximated by [21]

$$b_k = \log_2\left(1 + \frac{\text{SNR}_k}{\Gamma}\right), \tag{4}$$

where SNR_k denotes the SNR on the kth subcarrier, and the Γ is a constant ($\Gamma > 1$) which is directly related to the target BER (the larger Γ, the lower the BER will be). Note that we do not consider power loading in this paper. We assume all data-carrying subcarriers have the same average power. In VLC, because of the low-pass frequency response of LEDs, according to Eq. (4), more bits are allocated to low-frequency subcarriers and fewer bits are allocated to high-frequency subcarriers. Let us define the in-band subcarriers indices to be set $\mathcal{I} : [-N/2, N/2-1]$. Based on the number of bits loaded on each subcarrier, we divide the in-band subcarriers into a number of non-overlapped subsets; i.e., $\mathcal{I} = \mathcal{I}_1 \cup \mathcal{I}_2 \cup \cdots \cup \mathcal{I}_V$, where V is the number of subsets. Each subset of subcarriers are modulated by the same constellation type.

To summarize this section, Fig. 1 shows the bit-loaded OFDM system model in visible light communications.

III. PAPR REDUCTION

A. PAPR of VLC-OFDM

OFDM time-domain waveforms suffer from its high peak-to-average power ratio (PAPR), which is defined as [10]

$$\text{PAPR} \triangleq \frac{\max\limits_{0 \leq n \leq N-1} |x_n|^2}{\sigma_x^2}, \tag{5}$$

where σ_x^2 is the variance of x_n. Although PAPR is extensively studied in conventional RF-OFDM, we should use a different way to quantify the PAPR in VLC-OFDM because the time-domain signal is real-valued.

For the real-valued bipolar signal $\{x_n\}_{n=0}^{N-1}$, the square of the maximum value $\left(\max\limits_{0 \leq n \leq N-1} x_n\right)^2$ can be seen as the upper peak power, and the square of the minimum value $\left(\min\limits_{0 \leq n \leq N-1} x_n\right)^2$ can be seen as the lower peak power. We previously demonstrated that the performance of OFDM in VLC is directly related with upper PAPR (UPAPR) and lower PAPR (LPAPR) [12], [19], [22], where the UPAPR of x_n is defined as

$$\mathcal{U}(x_n) \triangleq \frac{\left(\max\limits_{0 \leq n \leq N-1} x_n\right)^2}{\sigma_x^2}, \tag{6}$$

and the LPAPR of x_n is defined as

$$\mathcal{L}(x_n) \triangleq \frac{\left(\min\limits_{0 \leq n \leq N-1} x_n\right)^2}{\sigma_x^2}. \tag{7}$$

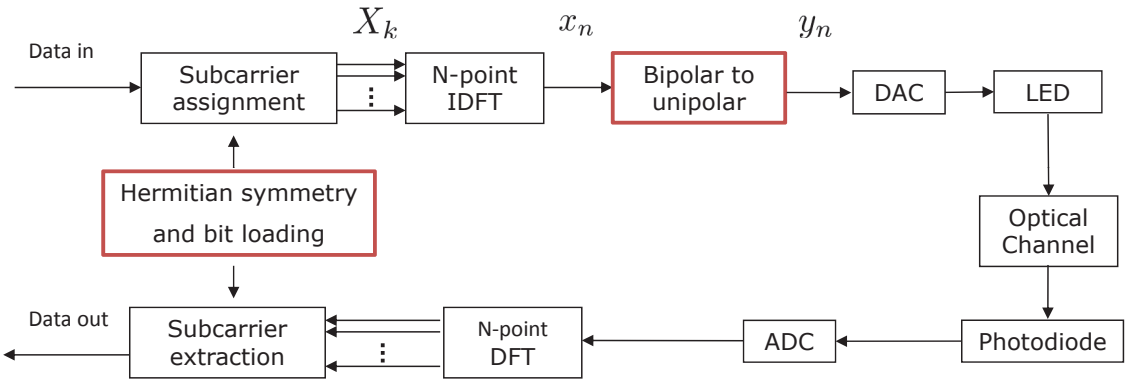

Fig. 1. Bit-loaded OFDM system model in visible light communications.

Large UPAPR and LPAPR make VLC-OFDM signals very sensitive to nonlinearity of LEDs [11]. Moreover, according to (3), high LPAPR requires large biasing B to convert the bipolar OFDM signal into unipolar version [12], which makes the system optical power inefficient. Based on the above motivations, we aim to reduce both UPAPR and LPAPR in VLC-OFDM system.

Because the biased signal y_n in Eq. (3) is limited by the dynamic range of LED $[I_L, I_H]$, the upper peak of x_n is in turn limited by $I_H - B$ and lower peak of x_n is limited by $I_L - B$, respectively. We can see that the upper PAPR and lower PAPR are not necessarily equally limited in VLC, depending on where the OFDM signal is biased. Note that biasing level is normally determined by illumination requirements. We define the asymmetric factor as

$$\varrho \triangleq \frac{(I_H - B)^2}{(I_L - B)^2}. \tag{8}$$

For example, $\varrho = 1$ dB means the upper PAPR is 1 dB less constrained than the lower PAPR.

Based on the independent and identically Gaussian distribution (i.i.d.) assumption of $\{x_n\}_{n=0}^{N-1}$ [23], we have derived the joint complementary cumulative distribution function (CCDF) of UPAPR and LPAPR in [19] as

$$\begin{aligned} & \text{CCDF}\{\mathcal{L}(x_n), \mathcal{U}(x_n), r, \varrho\} \\ \triangleq\ & 1 - Pr\{\mathcal{L}(x_n) \le r, \mathcal{U}(x_n) \le \varrho r\} \\ =\ & 1 - [\Phi(\sqrt{\varrho r}) - \Phi(-\sqrt{r})]^N. \end{aligned} \tag{9}$$

where r denotes the threshold, and $\Phi(\cdot)$ is the cumulative distribution function of the normal distribution.

Fig. 2 shows the simulated and theoretical joint CCDF of UPAPR and LPAPR of VLC-OFDM signals with $\varrho = 1$ dB and $N = 256, 1024$. Bit-loading and 4-QAM (no bit-loading) cases are considered in the simulations. The bit-loading schemes adopted in the simulations are shown in Table I and II. It can be seen that the simulated results match the theoretical values very well, and bit-loading does not affect the PAPRs joint distribution.

TABLE I. AN EXAMPLE OF BIT LOADING FOR DIFFERENT SUBCARRIERS SUBSETS ($N = 256$)

Subcarriers subset	Constellation type
$\mathcal{I}_1 = \{\pm 1, \pm 2, \ldots, \pm 10\}$	64-QAM
$\mathcal{I}_2 = \{\pm 11, \pm 12, \ldots, \pm 40\}$	16-QAM
$\mathcal{I}_3 = \{\pm 41, \pm 42, \ldots, \pm 127\}$	4-QAM

TABLE II. AN EXAMPLE OF BIT LOADING FOR DIFFERENT SUBCARRIERS SUBSETS ($N = 1024$)

Subcarriers subset	Constellation type
$\mathcal{I}_1 = \{\pm 1, \pm 2, \ldots, \pm 40\}$	64-QAM
$\mathcal{I}_2 = \{\pm 41, \pm 42, \ldots, \pm 160\}$	16-QAM
$\mathcal{I}_3 = \{\pm 161, \pm 162, \ldots, \pm 511\}$	4-QAM

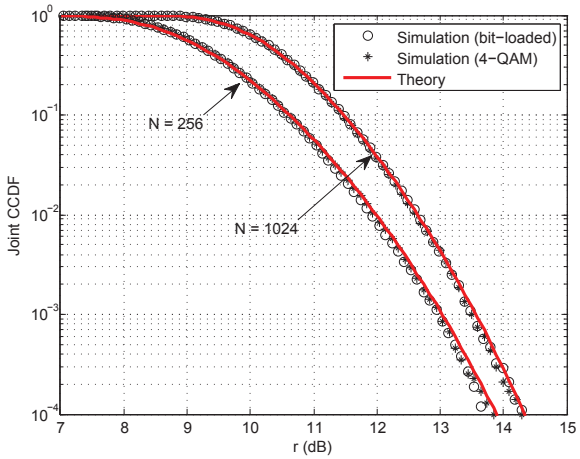

Fig. 2. Joint CCDF of UPAPR and LPAPR of VLC-OFDM signals with $\varrho = 1$ dB and $N = 256, 1024$.

B. Simple clipping

Clipping is the simplest way to reduce the UPAPR and LPAPR. Let c_u denote the upper clipping level and c_l denote the lower clipping level, the clipped signal is given by

$$\bar{x}_n = \begin{cases} c_u, & x_n > c_u \\ x_n, & c_l \le x_n \le c_u \\ c_l, & x_n < c_l \end{cases} \tag{10}$$

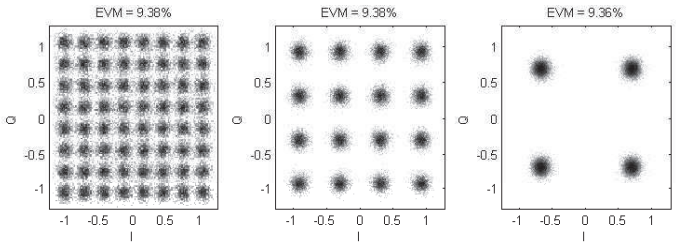

Fig. 3. Corrupted constellations and EVM with $\gamma_u = 7$ dB, and $\gamma_l = 6$ dB.

Note that c_u is positive and c_l is negative. Due to the asymmetric constraints, c_u is related with c_l as $c_u = -\sqrt{\varrho}c_l$.

Obviously, clipping yields to distortions and in turn degrades the system performance. Let us express the clipped signals as the original signals plus distortions d_n; i.e.,

$$\bar{x}_n = x_n + d_n. \tag{11}$$

Taking DFT of both sides of Eq. (11), the clipped signals in the frequency domain are obtained as

$$\bar{X}_k = X_k + D_k, \tag{12}$$

where D_k denotes the distortion on the kth subcarrier. Error vector magnitude (EVM) is a widely used figure of merit in literatures [7], [24] and standards [25] to quantify the in-band distortions, which is defined as

$$\text{EVM} \triangleq \sqrt{\frac{\sum_{k\in\mathcal{I}} E\{|D_k|^2\}}{\sum_{k\in\mathcal{I}} E\{|X_k|^2\}}}. \tag{13}$$

In communication standards, the EVM is regulated depending on constellation types. Intuitively, high order constellations are more sensitive to noises than lower order constellations. For example, in LTE standard [25], the EVM thresholds are 17.5% (4-QAM), 12.5% (16-QAM), and 8.0% (64-QAM), respectively. Therefore, for bit-loaded VLC-OFDM system, we should examine the constellation-wise EVM for different subcarriers subsets $\mathcal{I}_v$, which is defined as

$$\text{EVM}_{\mathcal{I}_v} \triangleq \sqrt{\frac{\sum_{k\in\mathcal{I}_v} E\{|D_k|^2\}}{\sum_{k\in\mathcal{I}_v} E\{|X_k|^2\}}}, v = 1, 2, \ldots, V. \tag{14}$$

As an example, we generate 1000 OFDM blocks according to the bit loading schemes shown in Table I. We choose the normalized lower clipping ratio $\gamma_l = c_l^2/\sigma_x^2 = 6$ dB, and the normalized upper clipping ratio $\gamma_u = c_u^2/\sigma_x^2 = 7$ dB. Fig. 3 shows the corrupted constellations after clipping for different subcarriers subsets (constellation types) and their corresponding constellation-wise EVMs. We can observe that the EVMs are at the same level (9.3 %), which means that the distortions are almost equally distributed on in-band subcarriers. However, uniform distribution of distortions is too "conservative" for low-order constellations. Ideally, given a certain amount of distortions, we would like to allocate more distortions to low-order modulations and less distortions to high-order modulations. However, with clipping, we cannot control the distribution of distortions in the frequency domain. The clipping ratios have to be chosen to meet the EVM requirements for all the modulation types.

C. Problem formulation

In this section, we will investigate the PAPR reduction problem for bit-loaded VLC-OFDM system. Let us consider a general distortion-based PAPR reduction setting

$$\tilde{X}_k = X_k + E_k, \quad k \in \mathcal{I}, \tag{15}$$

where E_k denotes the deliberately introduced distortions in the frequency domain and $\tilde{X}_k$ is the resulting signal in the frequency domain with lower PAPR. To ensure the resulting time-domain signal is real-valued, E_k must be Hermitian Symmetric; i.e., $E_k = E_{-k}^*$, $k = 1, 2, \ldots, N/2-1$, and E_0 and $E_{-N/2}$ must be real-valued. Moreover, to avoid DC wandering, the DC component should be zero; i.e., $E_0 = 0$.

In general, the more distortions allowed, the more PAPR reduction can be achieved. However, we must keep the introduced distortions under predefined thresholds to ensure reliable communications. In this paper, rather than placing a single EVM constraint on all in-band distortions as in references [15], [16], [18], we constrain distortions on different subcarriers sets (constellation types) with constellation-wise EVM thresholds. For each OFDM block, the constellation-wise EVM constraints can be written as

$$\sqrt{\frac{\sum_{k\in\mathcal{I}_v} |E_k|^2}{\sum_{k\in\mathcal{I}_v} |X_k|^2}} \le \epsilon_v, \quad v = 1, 2, \ldots V. \tag{16}$$

where ϵ_v denotes the EVM threshold for the subcarriers set $\mathcal{I}_v$.

Let $\{\tilde{x}_n\}_{n=0}^{N-1}$ denote the corresponding time-domain signal, which are the IDFT of $\{\tilde{X}_k\}_{k=-N/2}^{N/2-1}$, our objective is to find the distortions E_k to minimize the upper PAPR and lower PAPR for each OFDM block as

$$\underset{E_k}{\text{minimize}} \quad \max\{\mathcal{L}(\tilde{x}_n), \mathcal{U}(\tilde{x}_n)/\varrho\} \tag{17}$$

Note that in (17) we take asymmetric constraints for UPAPR and LPAPR (8) into account and put the inverse of asymmetric factor as the weight for upper PAPR. This objective function (17) can be further written as

$$\underset{E_k}{\text{minimize}} \quad r \tag{18}$$

$$\text{subject to} \quad \frac{\left(\min\limits_{0\le n\le N-1} \tilde{x}_n\right)^2}{\sum_{n=0}^{N-1} \tilde{x}_n^2} \le r, \tag{19}$$

$$\frac{\left(\max\limits_{0\le n\le N-1} \tilde{x}_n\right)^2}{\sum_{n=0}^{N-1} \tilde{x}_n^2} \le \varrho r \tag{20}$$

However, the constraints (19) and (20) are not convex. Following the pattern in reference [15], we relax the PAPR minimization problem (18-20) to a convex optimization problem

TABLE III. EVM CONSTRAINTS

Scenario	64-QAM	16-QAM	4-QAM
1	8 %	12.5 %	17.5 %
2	6 %	10 %	15 %

as

$$\begin{aligned} \underset{E_k}{\text{minimize}} \quad & g \\ \text{subject to} \quad & \left(\min_{0\le n\le N-1} \tilde{x}_n\right)^2 \le g, \\ & \left(\max_{0\le n\le N-1} \tilde{x}_n\right)^2 \le \varrho g, \\ & \sum_{k\in\mathcal{I}_v} \Re\{X_k^* E_k\} \ge -\epsilon_v^2 \sum_{k\in\mathcal{I}_v} |X_k|^2/2, \\ & v = 1, 2, \ldots V. \end{aligned} \tag{21}$$

Note that the r in (18) and the g in (22) are both intermediate variables that have no physical meanings.

As a summary, we formulate the PAPR minimization problem as follows:

$$\begin{aligned} \underset{E_k}{\text{minimize}} \quad & g \\ \text{subject to} \quad & \left(\min_{0\le n\le N-1} \tilde{x}_n\right)^2 \le g \\ & \left(\max_{0\le n\le N-1} \tilde{x}_n\right)^2 \le \varrho g \\ & \sum_{k\in\mathcal{I}_v} |E_k|^2 \le \epsilon_v^2 \sum_{k\in\mathcal{I}_v} |X_k|^2 \\ & \sum_{k\in\mathcal{I}_v} \Re\{X_k^* E_k\} \ge -\epsilon_v^2 \sum_{k\in\mathcal{I}_v} |X_k|^2/2 \\ & \tilde{x}_n = x_n + e_n, \quad e_n = \text{IFFT}(E_k) \\ & E_k = E_{-k},\ k = 1, 2, \ldots, N/2-1 \\ & E_0 = 0,\ E_{-N/2} \in \Re \\ & v = 1, 2, \ldots V,\ n = 0, 1, \ldots, N-1 \end{aligned} \tag{22}$$

To solve the quadratically constrained linear optimization problem (22), we used CVX, a package for specifying and solving convex programs [26]. A customized interior point method can be developed for real-time implementation [17], [27].

IV. NUMERICAL RESULTS

In this section, we provide numerical results by simulating the proposed convex optimization based PAPR reduction method for bit-loaded VLC-OFDM systems.

In the simulation, 20000 VLC-OFDM blocks were generated with $N = 256$ and bit loading scheme shown in Table I. Table III lists two scenarios of EVM constraints that we considered in simulations. Scenario 1 is based on LTE standard and scenario 2 places more limitations. We assume the asymmetric factor ϱ is 1 dB.

Fig. 4 compares the joint CCDF of UPAPR and LPAPR of original OFDM signals and the one of signals after proposed PAPR reduction. More than 6 dB PAPR reduction can be achieved for scenario 1 and more than 5.5 dB PAPR reduction can be achieved for scenario 2. Fig. 5 shows the constellations of OFDM signals after PAPR reduction for two scenarios. We can observe that all EVMs satisfy the designated constellation-wise constraints. Our proposed scheme can allocate more distortions to lower order constellations, and less distortions to higher order constellations, which is desired for bit-loaded OFDM systems. In the distortion-based PAPR reduction schemes, the introduced distortions can be treated as "resources" and should be wisely leveraged.

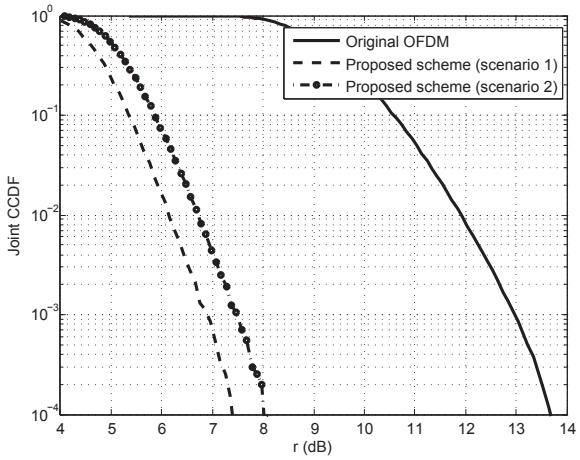

Fig. 4. Joint CCDF of UPAPR and LPAPR of VLC-OFDM signals with $\varrho = 1$ dB and $N = 256$.

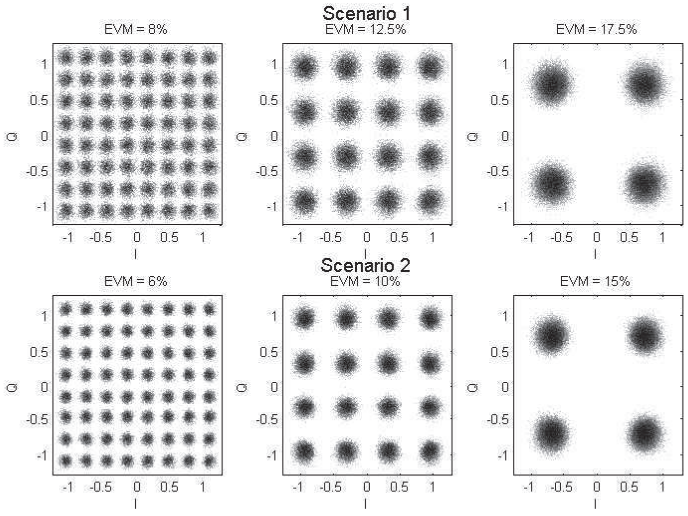

Fig. 5. Constellations and EVM of OFDM signals with proposed PAPR reduction.

V. CONCLUSIONS

In this paper, we reviewed the bit loaded visible light OFDM systems and analyzed the joint distribution of upper PAPR and lower PAPR. We proposed a distortion based method to reduce the upper PAPR and lower PAPR in bit-loaded VLC-OFDM systems. A quadratically constrained linear optimization problem was formulated to find the optimum distortions. Asymmetric constraints for upper PAPR and lower PAPR were considered in the formulation. We adopted constellation-wise EVM constraints, rather than a single one,

aiming to allocate less distortions to subcarriers with more bits loaded. The simulation results validate the proposed PAPR reduction scheme.

REFERENCES

[1] S. Rajagopal, Richard Roberts, and Sang-Kyu Lim, "IEEE 802.15.7 visible light communication: modulation schemes and dimming support," *IEEE Communications Magazine*, vol. 50, no. March, pp. 72–82, 2012.

[2] L. Grobe, A. Paraskevopoulos, J. Hilt, D. Schulz, F. Lassak, F. Hartlieb, C. Kottke, V. Jungnickel, and K.-D. Langer, "High-speed visible light communication systems," *IEEE Communications Magazine*, vol. 51, no. 12, pp. 60–66, 2013.

[3] A. Jovicic, J. Li, and T. Richardson, "Visible light communication: opportunities, challenges and the path to market," *IEEE Communications Magazine*, vol. 51, no. 12, pp. 26–32, 2013.

[4] Hoa Le Minh, Dominic O Brien, Grahame Faulkner, Lubin Zeng, Kyungwoo Lee, and Daekwang Jung, "100-Mb/s NRZ Visible Light Communications Using a Postequalized White LED," *IEEE Photonics Technology Letters*, vol. 21, no. 15, pp. 1063–1065, 2009.

[5] Steve Hranilovic, "On the design of bandwidth efficient signalling for indoor wireless optical channels," *International Journal of Communication Systems*, vol. 18, no. 3, pp. 205–228, Apr. 2005.

[6] Jean Armstrong, "OFDM for Optical Communications," *Journal of Lightwave Technology*, vol. 27, no. 3, pp. 189–204, Feb. 2009.

[7] Zhenhua Yu, Robert J. Baxley, and G. Tong Zhou, "EVM and achievable data rate analysis of clipped OFDM signals in visible light communication," *EURASIP Journal on Wireless Communications and Networking*, vol. 2012, Oct. 2012.

[8] A. M. Khalid, G. Cossu, R. Corsini, P. Choudhury, and E. Ciaramella, "1-Gb/s Transmission Over a Phosphorescent White LED by Using Rate-Adaptive Discrete Multitone Modulation," *IEEE Photonics Journal*, vol. 4, no. 5, pp. 1465–1473, Oct. 2012.

[9] D. Tsonev, H. Chun, S. Rajbhandari, J. McKendry, S. Videv, E. Gu, M. Haji, S. Watson, A. Kelly, G. Faulkner, M. Dawson, H. Haas, and D. O'Brien, "A 3-Gb/s Single-LED OFDM-based Wireless VLC Link Using a Gallium Nitride μLED," *Photonics Technology Letters, IEEE*, vol. PP, no. 99, pp. 1, 2014.

[10] R. J. Baxley and G. T. Zhou, "Peak-to-Average Power Ratio Reduction," in *Digital Signal Processing Handbook*, Vijay Madisetti, Ed. CRC Press, 2nd edition, 2009.

[11] Raed Mesleh, Hany Elgala, and Harald Haas, "LED Nonlinearity Mitigation Techniques in Optical Wireless OFDM Communication Systems," *Journal of Optical Communications and Networking*, vol. 4, no. 11, pp. 865, Oct. 2012.

[12] Zhenhua Yu, Robert J. Baxley, and G. Tong Zhou, "Peak-to-Average Power Ratio and Illumination-to-Communication Efficiency Considerations in Visible Light OFDM Systems," in *Proc. IEEE Intl. Conference on Acoustics, Speech, and Signal Processing (ICASSP)*, Vancouver, Canada, 2013.

[13] J. Armstrong, "Peak-to-average power reduction for OFDM by repeated clipping and frequency domain filtering," *Electronics Letters*, vol. 38, no. 5, pp. 246, Feb. 2002.

[14] R. J. Baxley, C. Zhao, and G. T. Zhou, "Constrained Clipping for Crest Factor Reduction in OFDM," *IEEE Transactions on Broadcasting*, vol. 52, no. 4, pp. 570–575, Dec. 2006.

[15] A. Aggarwal and T. H. Meng, "Minimizing the peak-to-average power ratio of OFDM signals using convex optimization," *IEEE Transactions on Signal Processing*, vol. 54, no. 8, pp. 3099–3110, Aug. 2006.

[16] Qijia Liu, Robert J. Baxley, Xiaoli Ma, and G. Tong Zhou, "Error Vector Magnitude Optimization for OFDM Systems With a Deterministic Peak-to-Average Power Ratio Constraint," *IEEE Journal of Selected Topics in Signal Processing*, vol. 3, no. 3, pp. 418–429, June 2009.

[17] Zhenhu Yu, Robert J. Baxley, and G. Tong Zhou, "Generalized interior-point method for constrained peak power minimization of OFDM signals," in *Proc. IEEE International Conference on Acoustics, Speech and Signal Processing (ICASSP)*, Prague, Czech Republic, May 2011, pp. 3572–3575.

[18] Z. Yu, R. J. Baxley, and G. T. Zhou, "Time-domain impulse injection method for crest factor reduction of OFDM signals," in *Proc. IEEE Statistical Signal Processing Workshop (SSP)*. Aug. 2012, pp. 832–835, IEEE.

[19] Zhenhua Yu, Robert J. Baxley, and G. Tong Zhou, "Distributions of upper PAPR and lower PAPR of OFDM signals in visible light communications," in *Proc. IEEE Intl. Conference on Acoustics, Speech, and Signal Processing (ICASSP)*, Florence, Italy, 2014.

[20] Zhenhua Yu, Robert J. Baxley, and G. Tong Zhou, "Impulses Injection for PAPR Reduction in Visible Light OFDM Communications," in *Proc. IEEE Global Conference on Signal and Information Processing (GlobalSIP)*, Atlanta, GA, 2014, pp. 1–5.

[21] John M. Cioffi, *A Multicarrier Primer*, Amati Communications Corporation and Stanford University, 1991.

[22] Zhenhua Yu, Robert J. Baxley, and G. Tong Zhou, "Brightness Control in Dynamic Range Constrained Visible Light OFDM Systems," in *Proc. IEEE Wireless and Optical Communication Conference (WOCC)*, Newark, NJ, Mar. 2014, pp. 1–5.

[23] Hua Yu, Min Chen, and Gang Wei, "Distribution of PAR in DMT systems," *Electronics Letters*, vol. 39, no. 10, pp. 799, 2003.

[24] Sandeep Kowlgi, Paul Mattheijssen, Corinne Berland, and Tim Ridgers, "EVM considerations for convergent multi-standard cellular base-station transmitters," *2011 IEEE 22nd International Symposium on Personal, Indoor and Mobile Radio Communications*, , no. 1, pp. 1865–1869, Sept. 2011.

[25] D. Astely, E. Dahlman, A. Furuskar, Y. Jading, M. Lindstrom, and S. Parkvall, "LTE: the evolution of mobile broadband," *IEEE Communications Magazine*, vol. 47, no. 4, pp. 44–51, Apr. 2009.

[26] Michael Grant and Stephen Boyd, "CVX: Matlab software for disciplined convex programmingversion 2.0 beta," 2013.

[27] Charles Nader, Peter Handel, and Niclas Bjorsell, "Peak-to-Average Power Reduction of OFDM Signals by Convex Optimization: Experimental Validation and Performance Optimization," *IEEE Transactions on Instrumentation and Measurement*, vol. 60, no. 2, pp. 473–479, Feb. 2011.